VARIATIONS OF NUSSELT NUMBERS IN A PROBLEM OF NATURAL CONVECTION IN ENCLOSURES

Viviana Cocco Mariani, viviana.mariani@pucpr.br
Graduate Program in Mechanical Engineering
Pontifical Catholic University of Parana – PUCPR
Rua Imaculada Conceição, 1155, Prado Velho, 80215-901, Curitiba, PR, Brazil

Adriano da Silva , adriano@unochapeco.edu.br
Center of Environmental Sciences of Foods
Regional Comunitary University of Chapeco - UNOCHAPECO
Rua Senador Atilio Fontana, 591 E, 89809-000, Chapecó, SC, Brazil

Abstract. *A two-dimensional solution for steady natural convection in enclosures partially open with a body generating heat is presented. An analysis is made based on two aspects of the radius, H/W = 1 and 2. The left and right walls are maintained at different constant temperatures while upper and bottom walls are thermally insulated. The physical model considered here are enclosures that have an opening on the right wall and a heating source located on the bottom or left vertical walls, occupying three different positions. Numerical simulations were performed for several values of the Rayleigh number (Ra_e) in the range between 10^3 and 10^6, while the intensity of the two effects – the difference in temperature of the vertical walls and the internal heating source (Ra_i) – was evaluated based on the relation $R = Ra_i/Ra_e$, in the range between 0 and 2500. In addition, simulation results for the local and average Nusselt numbers on the heated and colded walls of the enclosures are presented and discussed for different values of the parameters R, Ra_e, W_H and H/W. It is founded that the parameters modifications have significant effects on the average and local Nusselt number of the enclosures*

Keywords*: Natural convection, open enclosures, Nusselt number, Rayleigh number, heated source*

1. INTRODUCTION

Can to classify two elementary classes of natural convection flows in enclosures. The first is a vertical cavity with two vertical walls at different temperatures and with adiabatic horizontal surfaces. Natural convection flows in a vertical cavity are probably the most considered configuration in the studies of natural convection because of their relative simplicity and practical importance. Two-dimensional and three-dimensional numerical analysis for a vertical cavity with and without a body at the center has been performed in the past over a wide range of Rayleigh numbers. The second class of natural convection flows is a horizontal cavity with heating from below. Natural convection in a horizontal layer of fluid is relevant in practical problems of electronic equipment cooling, heat exchanger design, meteorology of the Earth's atmospheric boundary layers, and so on.

The study of natural convection in enclosures is important from both theoretical and practical points of view. The fluid dynamic behavior of air in open and closed environments with the presence or not of heat generating sources is extensively applicable in both industrial and residential environments. The interaction between the buoyancy and shear forces in partially open enclosures represent a physical problem found in a variety of industrial applications. The generation of heat inside the environment affects the characteristics of heat transfer associated with the flow field. Various studies have been dedicated to natural convection in closed and partially open enclosures, some of these studies are cited below.

Buoyancy-driven flows in rectangular enclosures arise frequently due to the horizontal temperature gradient caused by heating from the lowest surface or due to the vertical temperature gradient between two vertical surfaces held at different temperatures [1-7]. These studies investigate the effects of variation of temperature gradients, Rayleigh numbers, and aspect ratio on natural convection in enclosures. More recently the case of natural convection in closed enclosures has been analysed by Saeid [8] that investigated numerically the flow in two-dimensional cavity filled with a porous medium. It was found that the average Nusselt number increases with increasing amplitude of the hot wall temperature variation for all the values of Rayleigh number and different heat source length considered in the analysis. Peng *et al.* [9] studied natural convection in a three-dimensional cubic geometry heated differently on the two vertical walls. Corcione [10] studied the flow in closed rectangular two-dimensional domains with heated lower wall and cooled upper wall, investigating different boundary conditions on the lateral walls. Various simulations were carried out, varying the length of the enclosures and the Rayleigh number.

Considerable research has also been performed with various obstacles placed inside the enclosure. This research ([11]-[17]) revealed that these kinds of obstructions could change the characteristics of flow and heat transfer in the enclosure. Moreover, House *et al.* [18] examined the numerical effect of a centered, squared heat conducting on natural convection in a vertical square enclosure. They found that heat transfer across the enclosure may be modified due the thermal conductivity ratio less than or larger than unity. Oh *et al.* [19] investigated the steady flow inside the enclosure

drivened by two temperature differences: one across the enclosure and another caused by the heat source. They investigated the effects of Rayleigh number and temperature difference ratio. Ha *et al.* [20] studied the unsteady natural convection process when a temperature difference exists across the enclosure (right cold wall and left hot wall) and, at the same time a conducting generates heat within the enclosure using numerical procedures. They found that fluid flow in the enclosure grows with increasing *Ra*, increasing the convective heat transfer rate at the cold and hot wall. Ben-Nakhi and Chamkha [21] solved numerically steady, laminar, and natural convective fluid flow in a square enclosure with an inclined heated thin fin of arbitrary length attached to the hot wall. It was found that the Rayleigh number and the thin-fin inclination angle and length have significant effects on the average Nusselt number of the heated wall including the fin of the enclosure. Bazylak *et al.* [22] presented a computational analysis of the heat transfer due to an array of distributed heat sources on the bottom wall of a horizontal enclosure. Optimum heat transfer rates and the onset of thermal instability triggering various regimes are found to be governed by length and spacing of the sources and the width-to-height aspect ratio of the enclosure.

Some studies exist in enclosures with a side removed. Angirasa *et al.* [23] explored unsteady and steady numerical calculations for an isothermal cavity (all three sides heated). The underlying physical phenomena are explained in detail and Nusselt number data are provided. Earlier investigators ([24]-[26]) carried out numerical calculations in a domain that extended to far outside the cavity to determine the effect of the far field on the flow and heat transfer within the cavity. Large calculation and storage are required to obtain accurate solutions.

Indirectly related to the present study, Xia and Zhou [27] investigated a square and partially open enclosure with an internal source generating heat. These authors change the position on the bottom or left vertical walls only for three relations of *R*. Xia and Zhou [27] found that the opening presented advantageous to the flow and heat transfer in the cavity. In this case, the characteristics of flow and heat transfer were change with heated source location, external and internal Rayleigh number, and opening size. Reinehr *et al*. [28] examined the natural convection using the aspect of ratio $H/W = 2$, with an internal source heating varying its position only on the bottom wall. In that work, no heat transfer result was reported and a limited number of Ra_e and relation *R* were also studied.

Hence the present work proposes a study of natural convection in two partially open rooms (enclosures) submitted by temperature difference between left and right walls and an internal heat conduction source, to which few results have heen reported in the literature. The enclosures present an opening in the cooled right vertical wall, while the left vertical wall is heated and the upper and lower walls are adiabatic. Natural convection is induced by the difference of temperature between the vertical walls, and it is represented by the Rayleigh number (Ra_e), and by an internal heat conduction source represented by the Rayleigh number (Ra_i), occupying approximately 1% of the enclosures volume. The study is conducted numerically under the assumption of steady laminar flow, for two different values of the width-to-height aspect ratio of the enclosure in 1 and 2, and the Rayleigh number based on the enclosure height in the range between 10^3 and 10^6, the relation $R = Ra_i/Ra_e$ is evaluated in the range between 0 and 2500, while the internal heat conduction source position is evaluated in 0.25, 0.5 and 0.75 on the bottom and left vertical walls. In this context, the influence in the flow patterns, the temperature distributions and the heat transfer rates are analyzed and discussed.

This paper is organized as follows. Section 1 presents a brief review of some of the reports found in the literature on flows inside enclosures, with particular focus on work involving natural convection. Section 2 presents the conservation equations of mass, momentum and energy in dimensionless form and the boundary conditions used in the work. Representative results illustrate the effects of relation *R* in the local and average Nusselt numbers on the heated and colded walls of the enclosures are presented and discussed in Section 3 for various Ra_e numbers, for different values of the parameters W_H and H/W. Lastly, Section 4 discusses our conclusions.

2. STATEMENT OF THE PROBLEM

To model the flow under study, we use the conservation equations for mass, momentun and energy for the flow two-dimensional, steady and laminar. For the moderate temperature difference considered in this work all the physical properties of the fluid, m, k and c_p, are considered constant except the density, in the buoyancy term, which obeys the Boussinesq approximation. In the energy conservation equation, we neglect the effects of compressibility and viscous dissipation. Thus, the dimensionless equations that govern the flow are,

$$\frac{\partial U}{\partial X}+\frac{\partial V}{\partial Y}=0\,, \tag{1}$$

$$U\frac{\partial U}{\partial X}+V\frac{\partial U}{\partial Y}=-\frac{\partial P}{\partial X}+Pr\left(\frac{\partial^2 U}{\partial X^2}+\frac{\partial^2 U}{\partial Y^2}\right), \tag{2}$$

$$U\frac{\partial V}{\partial X}+V\frac{\partial V}{\partial Y}=-\frac{\partial P}{\partial Y}+Pr\left(\frac{\partial^2 V}{\partial X^2}+\frac{\partial^2 V}{\partial Y^2}\right)+Ra_e\,Pr\,q\,, \tag{3}$$

$$U\frac{\partial q}{\partial X}+V\frac{\partial q}{\partial Y}=\left(\frac{\partial^2 q}{\partial X^2}+\frac{\partial^2 q}{\partial Y^2}\right)+R. \tag{4}$$

The definitions of the dimensionless parameters are listed in the section nomenclature. The fluid considered in the interior of the enclosures is the atmospheric air using the Prandtl number, Pr = 0.71. The Rayleigh number (Ra_e) is represented by the difference of temperature between the vertical walls, $10^3 \le Ra_e \le 10^6$. The intensity of heat produced by the source is represented by the Rayleigh number (Ra_i), which is based on the volumetric heat generation rate. The influence of the intensity of the two Rayleigh numbers is evaluated by means of the relation,

$$R=\frac{Ra_i}{Ra_e}, \tag{5}$$

where $0 \le R \le 2500$.

The stream function is defined as

$$u = ?y/?y, \tag{6}$$

$$v = - ?y/?x, \tag{7}$$

but the numerical results illustrating the fluid's behavior are presented in terms of the dimensionless stream function given by

$$y_{dim}=\frac{y}{a}. \tag{8}$$

Other physical quantities of interest in the present study are the local and average Nusselt numbers along the hot and cold walls. These variables are defined, respectively, as

$$Nu=-\frac{\partial q}{\partial X}\Big)_w, \tag{9}$$

$$\overline{Nu_h}=-\int_0^H \frac{\partial q}{\partial X}\Big)_{X=0} dY, \tag{10}$$

$$\overline{Nu_c}=-\int_{H/2}^H \frac{\partial q}{\partial X}\Big)_{X=W} dY. \tag{11}$$

The fluid is investigated in two rectangular enclosures with length W and height H heated on the left vertical wall and cooled on the upper half of the right vertical wall. These two walls have a temperature prescribed, while the horizontal walls are adiabatic. The two-dimensional computational domain and the Cartesian system of co-ordinates used here are illustrated in Fig. 1. The position W_H (= 0.25, 0.5 and 0.75) illustrated in Fig. 1 is the distance considered, for example, from the left-hand lateral wall to the center of the heating source. The internal heat source is located on the bottom or left vertical walls at different places and it is occupying 1% of the total volume of the enclosures, e.g., occupying 4x4 control volumes of the enclosures. The lower half of the right wall is open and is in contact with the air outside of the enclosure. The boundary conditions used are,

$U = V = 0$ and $q = 1$ at $X = 0$ and $0 \le Y \le H$, (12a)
$U = V = 0$ and $q = 0$ at $X = W$ and $H/2 \le Y \le H$, (12b)
$U = V = 0$ and $\partial q/\partial Y = 0$ at $0 \le X \le W$ and $Y = 0$, (12c)
$U = V = 0$ and $\partial q/\partial Y = 0$ at $0 \le X \le W$ and $Y = H$, (12d)
$K\,\partial q_s/\partial n = \partial q_f/\partial n$ at the source-fluid interfaces, (12e)

where K is the ratio of the thermal conductivities between the heated source and the fluid, q_s is the dimensionless temperature in the heated source and q_f is the dimensionless temperature in the fluid.The velocity and temperature profiles in the opening are assumed as,

if $U > 0$ then $\partial q/\partial X = 0$ else $q = 0$, $V = 0$ at $X = W$ and $0 \le Y \le H/2$. (13)

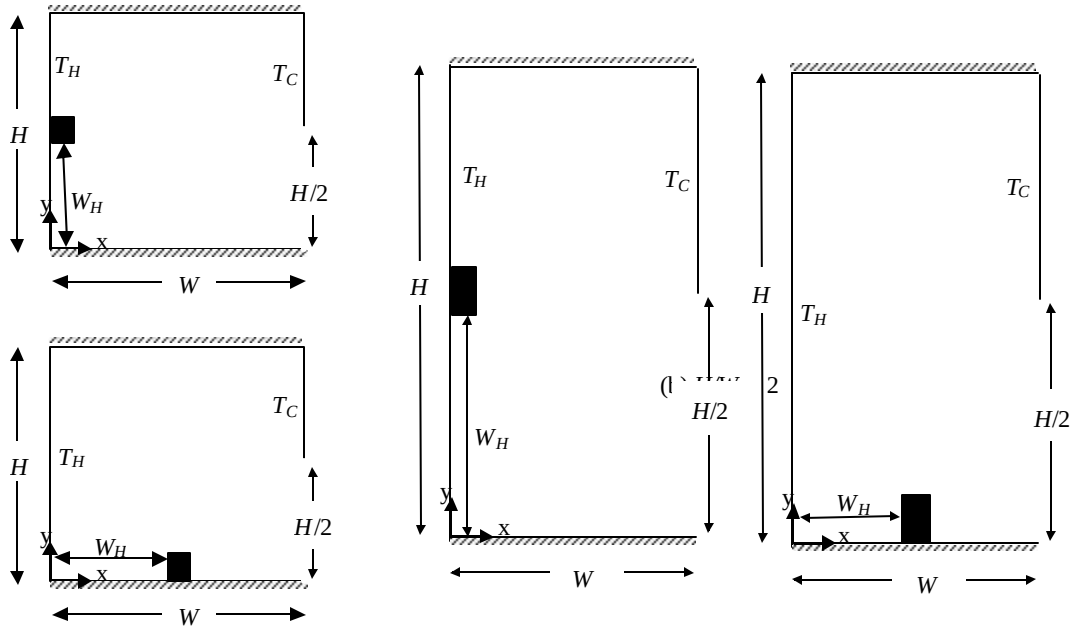

Figure 1. Geometries employed.

The differential equations, represented by equations (1) to (4), together with respective boundary conditions, equations (12) to (13), are solved using the Finite Volume Method described in Patankar [29]. In this method, the solution domain is divided in small finite control volumes. The differential equations are integrated to each of those control volumes. From this integration there were algebraic equations as a result which, when solved, simultaneously or separately, supplied pressure and velocity components. A power law scheme is adopted for the convection-diffusion formulation. For the coupling pressure-velocity the SIMPLEC algorithm (*Semi Implicit Method for Pressure Linked Equations Consistent*) is used [29].

The discretized equations are solved iteratively, using the line by line method known as Thomas algorithm or TDMA (*TriDiagonal Matrix Algorithm*). An under-relaxation parameter of 0.5 was used in order to obtain a stable convergence for the solution of momentum and energy equations while there was no need for such a parameter in the solution of pressure equation.

The validation of computer code of this work has been verified for the natural convection problem in an enclosure closed without a heat conduction source. The results presented here are for two Rayleigh numbers, $Ra_e = 10^5$ and $Ra_e = 10^6$. Hortman *et al.* [5] found the average Nusselt numbers 4.616 and 4.525 for $Ra_e = 10^5$ and grids 42 x 42 and 82 x 82, respectively, while in our study were found 4.604 and 4.535, respectively. For the $Ra_e = 10^6$, they found the average Nusselt numbers 9.422 and 8.977 for the same grids, while in our study were found 9.487 and 8.975, respectively.

Grid-independence tests have been conducted for all the configurations studied in this work. Three different grid sizes (22 x 22, 42 x 42 and 82 x 82) were used. Because of the minor differences for 42 x 42 and 82 x 82 grids, the 42 x 42 uniform grid is chosen for all the simulations presented in this work. Staggered storage of the variables is used. The numerical solution is considered to be converged when the maximum absolute value of the mass conservation is smaller than 10^{-10}.

3. RESULTS AND DISCUSSION

In order to compare the numerical code specifically developed for the present study, some solutions obtained in square cavity, $W/H = 1$, when the internal heat-conduction source is centrally located on the bottom wall (in the position $W_H = 0.5$) have been compared with results of Xia and Zhou [27] and Reinehr *et al.* [28], showing a good agreement. Such results are presented in Tab. 1, where occur different flow patterns with changing of Ra_e or R. The comparative analysis between the values of Tab. 1 denote that relative deviation (RD),

$$RD = \left(100.|Dq_{max}|/q_{max}\right)\% \tag{14}$$

where θ_{max} is value proposed in Xia and Zhou [27] or Reinehr *et al.* [28] as the case, and Dq_{max} is the difference between the results of this work and of two mentioned works. The results of Xia and Zhou [27] are situated in the interval of

3.11% ≤ RD ≤ 8.3% while for Reinehr *et al*. [28] the interval is 0.2% ≤ RD ≤ 7%, showing a good agreement between the results.

Table 1. Maximum dimensionless temperature (q_{max}) for H/W = 1 and W_H = 0.5.

Parameters	Xia and Zhou [27]	Reinehr *et al.* [28]	Present work
R = 400, $Ra_e = 10^5$	1.80	1.82	1.95
R = 1000, $Ra_e = 10^5$	3.90	4.07	4.19
R = 2500, $Ra_e = 10^3$	15.40	15.69	16.08
R = 2500, $Ra_e = 10^4$	10.90	11.50	11.47
R = 2500, $Ra_e = 10^5$	8.30	8.46	8.56
R = 2500, $Ra_e = 10^6$	6.10	-	6.29

The maximum dimensionless temperature increases considerably with the increase of the relation R, keeping Ra_e constant, according to Tables 2 and 3, independent from the position of the heat source and from the geometric relation H/W. The maximum dimensionless temperature decreases with the increasing of the Ra_e when the number R is kept constant. A comparison of the maximum dimensionless temperatures at the same values of R and Ra_e, with the heat source in different positions inside the enclosures, indicates that the differences are not significant. When the heated source is located at the hot wall (left vertical wall), it can be seen by comparing the dimensionless temperature in Tables 2 and 3 that there are decreasing and increasing for the majority of the cases, respectively, for H/W = 1 and 2 in relation the heated source located on the bottom wall. In Tables 4 to 5, note that the increase in the intensity of the fluid dynamic flow is less pronounced with the increase in the relation R for the same Ra_e than that observed with the increase of Ra_e for the same relation of R at both H/W = 1 and H/W = 2. A comparison of the maximum and minimum values of the dimensionless flow function for the same R and Ra_e values with the heat source in different positions inside the enclosure, reveals that the differences are irrelevant.

Table 2. Maximum dimensionless temperature for H/W = 1.

Parameters		Positions					
		W_H = 0.25		W_H = 0.5		W_H = 0.75	
R	Ra_e	Bottom	Left	Bottom	Left	Bottom	Left
400	10^3	3.241	1.667	3.458	1.674	2.954	1.707
	10^4	2.648	1.545	2.595	1.595	2.426	1.664
	10^5	2.018	1.379	1.905	1.468	1.828	1.565
	10^6	1.496	1.253	1.348	1.321	1.331	1.432
1000	10^3	6.900	2.787	7.590	2.786	6.989	2.839
	10^4	5.541	2.586	5.590	2.636	5.476	2.739
	10^5	4.146	2.297	4.157	2.385	4.096	2.523
	10^6	3.043	1.976	2.956	2.093	2.898	2.254
2500	10^3	15.279	5.556	16.080	5.543	15.040	5.654
	10^4	11.913	5.118	11.467	5.179	11.341	5.383
	10^5	8.492	4.496	8.553	4.599	8.576	4.822
	10^6	6.304	3.852	6.286	3.983	6.114	4.164

Table 3. Maximum dimensionless temperature for H/W = 2.

Parameters		Positions					
		W_H = 0.25		W_H = 0.5		W_H = 0.75	
R	Ra_e	Bottom	Left	Bottom	Left	Bottom	Left
400	10^3	1.787	1.963	1.767	2.003	1.317	2.052
	10^4	1.591	1.806	1.547	1.865	1.181	1.945
	10^5	1.251	1.603	1.109	1.694	1.000	1.789
	10^6	1.000	1.419	1.000	1.513	1.000	1.632
1000	10^3	3.364	3.555	3.667	3.606	2.921	3.693
	10^4	2.960	3.207	3.205	3.275	2.734	3.399
	10^5	2.355	2.808	2.385	2.915	2.247	3.054
	10^6	1.795	2.442	1.686	2.575	1.545	2.718
2500	10^3	7.297	7.409	8.342	7.490	6.899	7.705
	10^4	6.146	6.587	6.828	6.691	6.338	6.925
	10^5	4.770	5.692	4.808	5.838	4.799	6.083
	10^6	3.298	4.963	3.255	5.131	3.150	5.311

Table 4. Minimum and maximum dimensionless stream function for $H/W = 1$ with heat generation source on the bottom wall.

Parameters		Positions		
R	Ra_e	$W_H = 0.25$	$W_H = 0.5$	$W_H = 0.75$
400	10^3	-1.995; 0.038	-1.660; 0.130	-1.060; 0.016
	10^4	-7.972; 0.183	-8.226; 0.145	-7.767; 0.028
	10^5	-13.871; 0.460	-14.674; 0.511	-14.598; 0.474
	10^6	-22.142; 2.256	-26.934; 3.619	-27.260; 3.609
1000	10^3	-3.052; 0.117	-2.752; 0.818	-0.934; 1.380
	10^4	-10.566; 0.586	-11.305; 1.635	-8.712; 4.576
	10^5	-18.613; 2.043	-20.793; 1.884	-22.416; 1.314
	10^6	-27.362; 5.406	-31.242; 5.561	-32.331; 5.641
2500	10^3	-4.994; 0.292	-4.416; 2.663	-1.848; 4.490
	10^4	-14.299; 1.337	-14.279; 5.922	-8.114; 12.097
	10^5	-25.208; 3.944	-28.213; 5.275	-31.510; 6.170
	10^6	-37.989; 8.868	-42.773; 10.392	-45.252; 8.493

Table 5. Minimum and maximum dimensionless stream function for $H/W = 2$ with heat generation source on the bottom wall.

Parameters		Positions		
R	Ra_e	$W_H = 0.25$	$W_H = 0.5$	$W_H = 0.75$
400	10^3	-0.389; 0.002	-0.359; 0.006	-0.358; 0.0004
	10^4	-3.538; 0.017	-3.461; 0.023	-3.376; 0.0046
	10^5	-12.109; 0.037	-12.453; 0.073	-12.807; 0.155
	10^6	-20.598; 0.510	-21.193; 1.535	-21.552; 2.381
1000	10^3	-0.457; 0.006	-0.376; 0.039	-0.340; 0.0147
	10^4	-4.202; 0.051	-4.172; 0.238	-3.635; 0.051
	10^5	-13.831; 0.289	-14.825; 0.852	-14.861; 0.572
	10^6	-23.062; 1.376	-24.018; 3.458	-24.657; 5.583
2500	10^3	-0.695; 0.019	-0.664; 0.151	-0.3815; 0.169
	10^4	-5.864; 0.137	-6.184; 0.788	-5.004; 0.801
	10^5	-17.616; 0.873	-19.416; 2.761	-19.823; 2.607
	10^6	-27.374; 3.772	-30.054; 5.301	-34.470; 9.599

Figs. 11a and 11b show the convective heat transfer, represented by the local Nusselt along the hot and cold walls, respectively, for the square cavity at various R, i.e., various intensity of internal heat conduction source located in the center of bottom wall. For the hot wall, Nu increases almost monotonically with distance Y along the wall for $R < 1000$. On the other hand, Nu passes through a minimum and then a maximum in $Y = 0.25$ for $R > 1000$, such behavior is determined by the intensity of eddies between the heat source and heated wall. It is verified that Nu_h increases when the approaches of the upper wall this occurs due the increasing of secondary eddy moves the position of the maximum gradient for the top of cavity, as show the Figs. 4 and 5. For the cold wall, Nu increases with R, because the increase in the value of R causes an increase in the flow intensity and soon increases the temperature gradient next to the cold wall. The Nu_c is maximum in the position $Y = 0.5$, region of bigger temperature gradient, and increases along the cold wall.

Figs. 12a and 12b show the local Nusselt along the hot and cold walls, respectively, for the square cavity at various Ra_e for internal heat conduction source located in the center of bottom wall. For the hot wall, Nu decreases monotonically since $Y = 0$ even approximately $Y = 0.35$ for $Ra_e > 10^3$ after increases with the distance Y along the hot wall. For $Ra_e < 10^3$ the Nu_h increases along the hot wall as Y increases. These behaviors of variation of the Nu can be attributed to the formation of secundary eddies and their decreasing size with increase for Ra_e. It is observed that for $Ra_e \geq 5000$ the behavior of the Nu_c is little modified this because the flow patterns also does not changed. The average Nu on the hot and cold walls are shown in Figs. 13a and 13b, respectively, for $W_H = 0.5$ and $H/W = 1$ for generation heat in bottom and in Figs. 13c and 13d for generation heat in left vertical wall, as a function of R and Ra_e. As shown in the isotherms of Figs. 5 and 7 the fluid temperature increases with increasing of R in the square enclosure and decreases with increasing of Ra_e. Thus the temperature gradient on the hot wall decreases with increasing of R and increases with increasing of Ra_e giving, respectively, decreasing and increasing at Nu_h as shown in Figs. 13a and 13c. In these figures for approximately $R > 400$ the Nu_h has negative values, meaning that the fluid temperature next to the hot wall is larger than the hot wall temperature and the net heat flow at the hot wall changes its direction from the enclosure to the hot wall. Figs. 13b and 13d show that Nu_c increases with increasing of Ra_e and R, meaning that the heat flow from the enclosure to the cold wall increases with the increasing this parameters. For example, Nu_c and Nu_h for $Ra_e = 10^4$ are larger than those for $Ra_e = 10^3$ for the same R due to increasing convective heat transfer with increasing Ra_e.

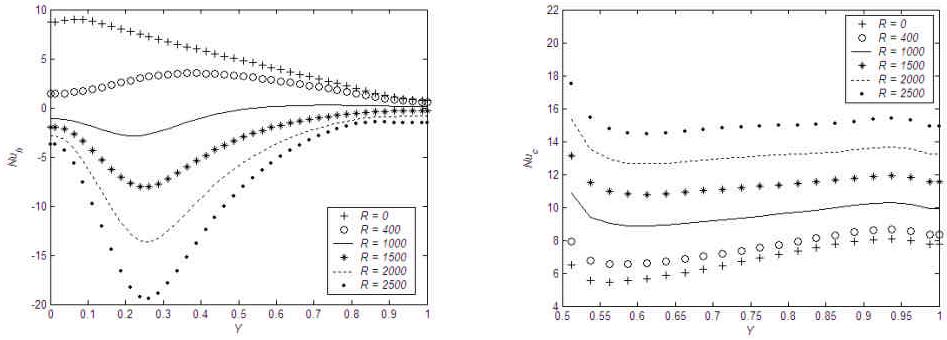

(a) (b)

Figure 11. Local Nusselt number along the (a) hot and (b) cold walls vs. R, for $Ra_e = 10^5$; generation heat in bottom wall, $W_H = 0.5$ and $H/W = 1$.

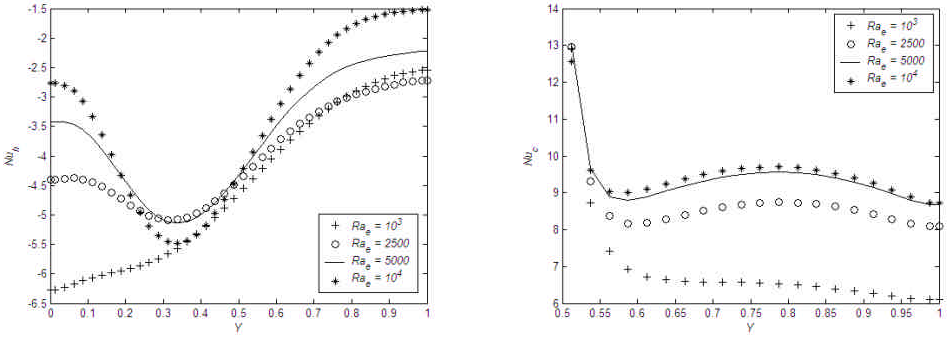

(a) (b)

Figure 12. Local Nusselt number along the (a) hot and (b) cold walls vs. Ra_e, for $R = 10^3$; generation heat in bottom wall, $W_H = 0.5$ and $H/W = 1$.

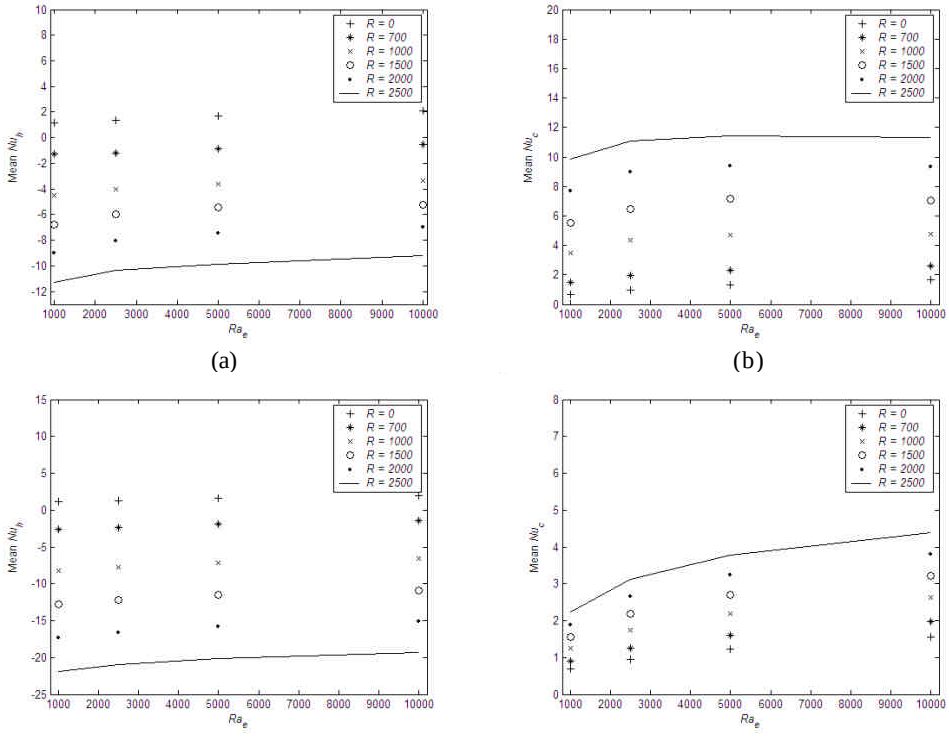

(a) (b)

(c) (d)

Figure 13. Variation of mean Nusselt with R and Ra_e, (a) Nu_h and (b) Nu_c for generation heat in bottom wall and (c) Nu_h and (d) Nu_c for generation heat in left vertical wall, $W_H = 0.5$ and $H/W = 1$.

Figs. 14a and 14b show the average Nu at the hot and cold walls, respectively for W_H = 0.5 and H/W = 2 for generation heat in bottom wall. Figs. 14c and 14d show the sam e results for the generation heat in left vertical wall. Comparing the Figs. 13a and 13b and Figs. 13c and 13d with Figs. 14a and 14b and Figs. 14c and 14d, respectively, can be observed that Nu_h in this last figure has the value almost duplicate with relation the first figure. In Fig. 14c, the Nu_h decreases with increasing R due to increased effects of temperature difference caused by heat generation. However, in Fig. 14d, the Nu_c maintains its level with increasing of R because the fluid flow direction is the same as the heat flow direction. Fig. 14b shows that Nu_c increases with increasing of Ra_e and R, meaning that the heat flow from the enclosure to the cold wall increases with the increasing this parameters. However, for $R > 1500$ and $Ra_e < 5.10^3$, the Nu_c decreases with increasing of these parameters.

The Figs. 15a and 15b give the variation of average Nu_h and Nu_c, respectively, with the location of heating source. With the heated source moving on the hot wall (vertical wall) or on the adiabatic wall (horizontal wall) occur some changes in the average Nusselt number. When the heating source is located near the opening the enclosures on the bottom wall Nu_h is maximum for square cavity, while Nu_c is maximum for heated source located in the middle region of horizontal wall for retangular cavity.

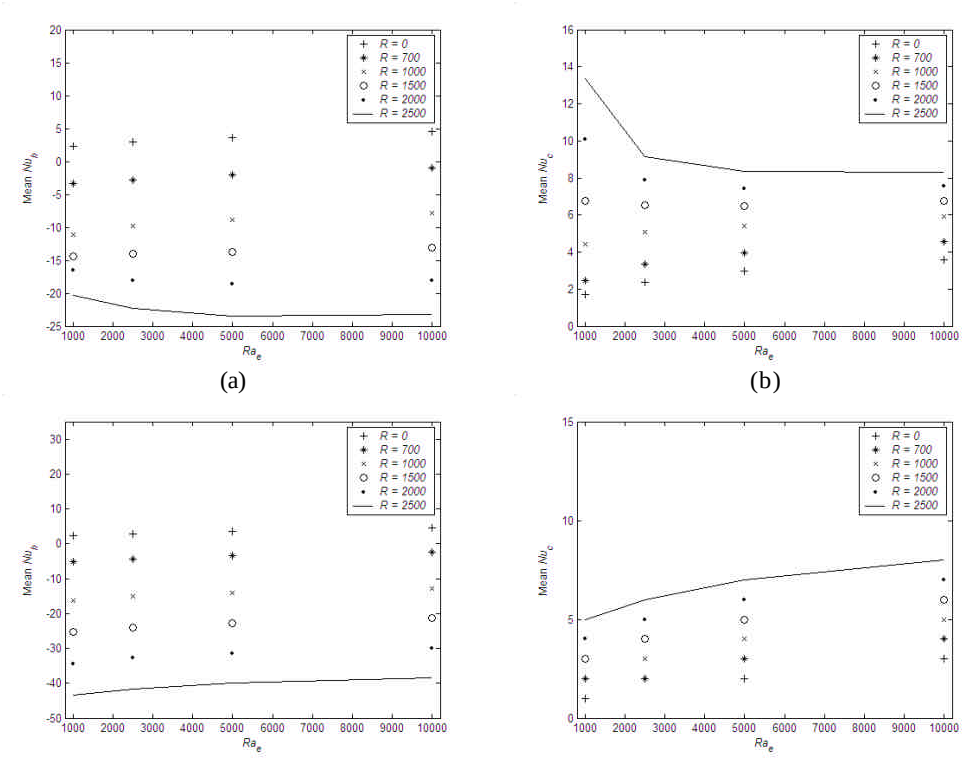

Figure 14. Variation of mean Nusselt with R and Ra_e, (a) Nu_h and (b) Nu_c for generation heat in bottom wall and (c) Nu_h and (d) Nu_c for generation heat in left vertical wall, W_H = 0.5 and H/W = 2.

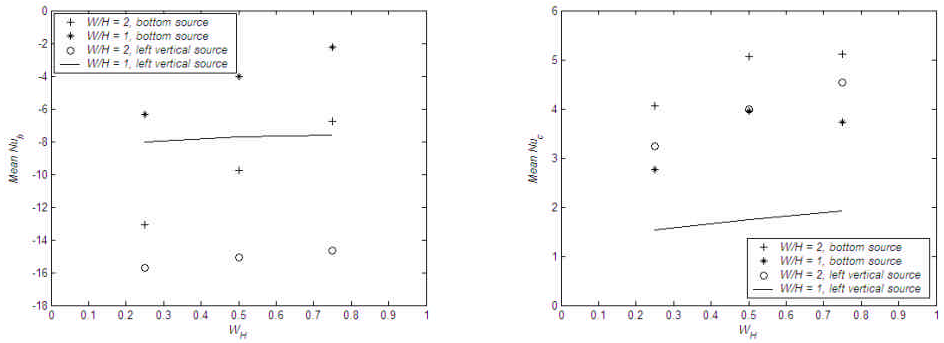

Figure 15. Variation of mean (a) Nu_h and (b) Nu_c with the position W_H for R = 1000 and Ra_e = 2500.

4. CONCLUSIONS

The present study investigates the variations of maximum temperatures and maximum and minimum stream function streamlines as a function of different values of internal and external Rayleigh numbers, R and Ra_e, for enclosures with two aspects of the radius, H/W = 1 and 2. When Nu_h has negative values it shows that the fluid temperature close to the hot wall is larger than the hot wall temperature and the net heat flow at the hot wall changes its direction from the enclosure to the hot wall. When R has a small value, the heat transfer and flow in the enclosure during the transient process maintain the natural convective mode, which is governed by the temperature difference between the hot and cold walls. But when R has a large value, the mode of heat transfer and flow are changed from the natural convection governed by the temperature difference between the hot and cold wall to that caused by heat generation. Fluid flow in the enclosure increases with increasing Ra_e, increasing the convective heat transfer rate at the cold and hot walls. The Nu_h, Nu_c and local Nusselt profiles are influenced by Ra_e and R in both enclosures. The position of the heating source has influence on the flow and heat transfer in the enclosures. The heating source changes the flow and heat transfer mainly in the region above it but has negligible influence on those in the region below it. The H/W aspect ratio has significant influence in the results obtained.

5. REFERENCES

1. S. Ostrach and C. Raghaven, Effect of Stabilizing Thermal Gradients on Natural Convection in Retangular Enclosures, *ASME Journal of Heat Transfer* , vol. 101, no. 2, pp. 238-243, 1979.
2. G. de Vahl Davis, Natural Convection of Air in a Square Cavity: A Benchmark Solution, *International Journal for Numerical Methods in Fluids* , vol. 3, no. 3, pp. 249-264, 1983.
3. K. T. Yang, Natural Convection in Enclosures, in *Handbook of Single Phase Convection Heat Transfer*, Wiley, New York, NY, 1987.
4. S. Ostrach, Natural Convection in Enclosures, *ASME Journal of Heat Transfer*, vol. 110, pp. 1175-1190, 1988.
5. M. Hortmann, M. Peric, and G. Scheuerer, Finite Volume Multigrid Prediction of Laminar Natural Convection: Benchmark Solutions, *International Journal for Numerical Methods in Fluids*, vol. 11, no. 2, pp. 189-207, 1990.
6. P. Le Quére, Accurate Solutions to the Square Thermally Driven Cavity at High Rayleigh Number, *Computers Fluids*, vol. 20, no. 1, pp. 29-41, 1991.
7. O. Aydin, A. Unal, and T. Ayhan, Numerical Solutions for Buoyancy-Driven Flow in a 2D Square Enclosure Heated from one Side and Cooled from Above, *Proceedings of the Advances in Computational Heat Transfer Symposium*, Begell House, New York, NY, pp. 387–394, 1997.
8. N. H. Saeid, Natural Convection in Porous Cavity with Sinusoidal Bottom Wall Temperature Variation, *International Communications in Heat and Mass Transfer*, vol. 32, no. 3-4, pp. 454-463, 2005.
9. Y. Peng, C. Shu, and Y. T. Chew, A 3D Incompressible Thermal Lattice Boltzmann Model and its Application to Simulate Natural Convection in a Cubic Cavity, *Journal of Computational Physics*, vol. 193, no. 1, pp. 260–274, 2003.
10. M. Corcione, Effects of the Thermal Boundary Conditions at the Sidewalls Upon Natural Convection in Rectangular Enclosures Heated from Below and Cooled from Above, *International Journal of Thermal Sciences*, vol. 42, no. 2, pp. 199-208, 2003.
11. H. H. Chu, and S. W. Churchill, The Effect of Heater Size, Location, Aspect-Ratio and Boundary Conditions on Two-Dimensional Laminar Natural Convection in Rectangular Channels, *Journal of Heat Transfer*, vol. 98, no. 2, pp. 194-201, 1976.
12. A. Khalilollahi, and B. Sammakia, Unsteady Natural Convection Generated by a Heated Surface within an Enclosure, *Numerical Heat Transfer Part A*, vol. 9, no. 6, pp. 715-730, 1986.
13. M. Keyhani, V. Prasad, and R. Cox, An Experimental Study of Natural Convection in a Vertical Cavity with Discrete Heat Sources, *Journal of Heat Transfer*, vol. 110, no. 3, pp. 616-624, 1988.
14. B. Farouk, Turbulent Thermal Convection in an Enclosure with Internal Heat Generation, *Journal of Heat Transfer*, vol. 110, no. 1, pp. 126-132, 1988
15. C. J. Ho, and J. Y. Chang, A Study of Natural Convection Heat Transfer in a Vertical Rectangular Enclosure with Two-Dimensional Discrete Heating: Effect of Aspect Ratio, *International Journal of Heat and Mass Transfer*, vol. 37, no. 6, pp. 917-925, 1994.
16. Q. Deng, and G. Tang, Numerical Visualization of Mass and Heat Transport for Conjugate Natural Convection/Heat Conduction by Streamline and Heatline, *International Journal of Heat and Mass Transfer*, vol. 45, no. 11, pp. 2373-2385, 2002.
17. H. F. Oztop, I. Dagtekin, and A. Bahloul, Comparison of Position of a Heated Thin Plate Located in a Cavity for Natural Convetion, *International Communications in Heat and Mass Transfer* , vol. 31, no. 1, pp.121-132, 2004.

18. J. M. House, C. Beckermann, and T. F. Smith, Effect of a Centered Conducting on Natural Convection Heat Transfer in an Enclosure, *Numerical Heat Transfer Part A*, vol. 18, no. 2, pp. 213-225, 1990.
19. J. Y. Oh, M. Y. Ha, and K. C. Kim, Numerical Study of Heat Transfer and Flow of Natural Convection in an Enclosure with a Heat-Generating Conducting, *Numerical Heat Transfer Part A*, vol. 31, no. 3, pp. 289-304, 1997.
20. M. Y. Ha, M. J. Jung and Y. S. Kim, Numerical Study on Transient Heat Transfer and Fluid Flow of Natural Convection in an Enclosure with a Heat-Generating Conducting, *Numerical Heat Transfer Part A*, vol. 35, no. 4, pp. 415-433, 1999.
21. A. Ben-Nakhi and A. J. Chamkha, Effect of Length and Inclination of a Thin Fin on Natural Convection in a Square Enclosure, *Numerical Heat Transfer Part A*, vol. 50, no. 4, pp. 389-407, 2006.
22. A. Bazylak, N. Djilali, and D. Sinton, Natural Convection in an Enclosure with Distributed Heat Sources, *Numerical Heat Transfer Part A*, vol. 49, no. 7, pp. 655-667, 2006.
23. D. Angirasa, J. G. M. Eggels, and F. T. M. Nieuwstadt, Numerical Simulation of Transient Natural Convection from an Isothermal Cavity Open on a Side, *Numerical Heat Transfer Part A*, vol. 28, no. 6, pp. 755-768, 1995.
24. F. Penot, Numerical Calculation of Two-Dimensional Natural Convection in Isothermal Open Cavities, *Numerical Heat Transfer*, vol. 5, pp. 421-437, 1982.
25. P. Le Quére, J. A. C. Humphrey, and F. S. Sherman, Numerical Calculation of Thermally Driven Two-Dimensional Unsteady Laminar Flow in Cavities of Rectangular Cross Section, *Numerical Heat Transfer*, vol. 4, pp. 249-283, 1981.
26. Y. L. Chan and C. L. Tien, A Numerical Study of Two-Dimensional Natural Convection in Square Open Cavities, *Numerical Heat Transfer* , vol. 8, no. 3, pp. 65-80, 1985.
27. J. L. Xia, and Z. W. Zhou, Natural Convection in an Externally Heated Partially Open Cavity with a Heated Protrusion, FED-Vol. 143/HTD, vol. 232, *Measurement and Modeling of Environmental Flows – ASME*, pp. 201-208, 1992.
28. E. L. Reinehr, A. A. U. Souza and S. M. A. Souza, Comportamento Fluidodinâmico do Ar com Convecção Natural e Fonte de Geração de Calor em Ambiente Confinado. *XIV Congresso Brasileiro de Engenharia Química*, Natal, Rio Grande do Norte, Brasil, pp. 1-8, 2002, (in Portuguese).
29. S. V. Patankar, *Numerical Heat Transfer and Fluid Flow* , Hemisphere Washington, DC, 1980.

6. RESPONSIBILITY NOTICE

The authors are the only responsible for the printed m aterial included in this paper.